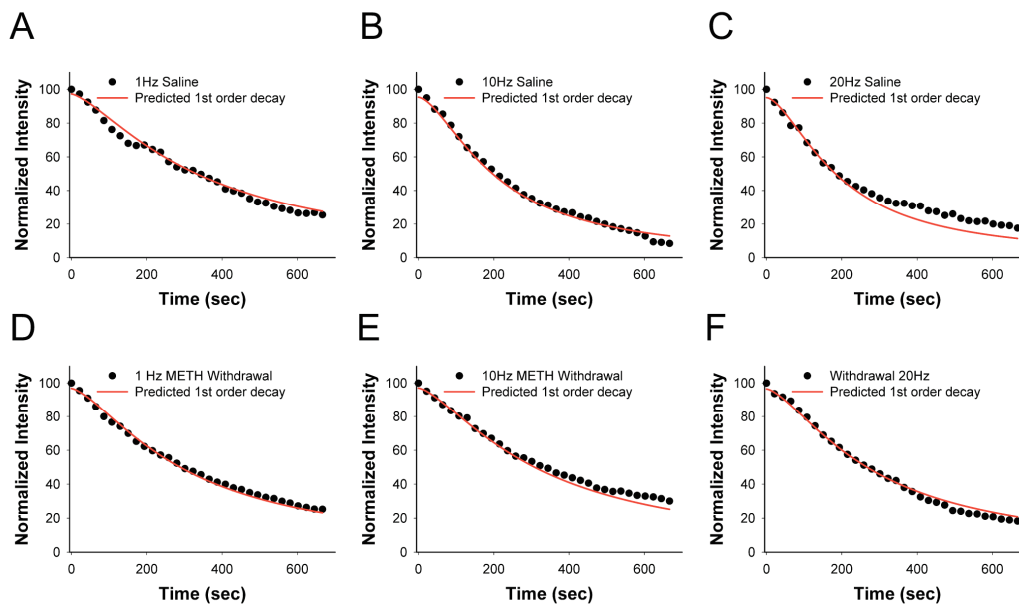


## Supplemental Data, Neuron, volume 58

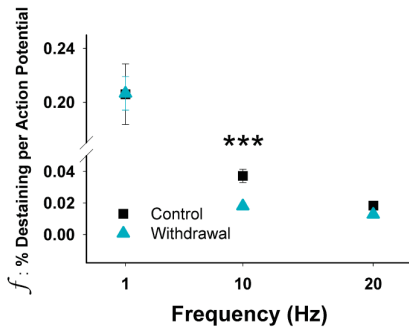
## Repeated methamphetamine causes long-lasting presynaptic corticostriatal depression that is renormalized with drug readministration

Nigel S. Bamford, Hui Zhang, John A. Joyce, Christine A. Scarlis, Whitney Hanan, Nan-Ping Wu, Véronique M. André, Rachel Cohen, Carlos Cepeda, Michael S. Levine, Erin Harleton, and David Sulzer

## Supplemental Figures

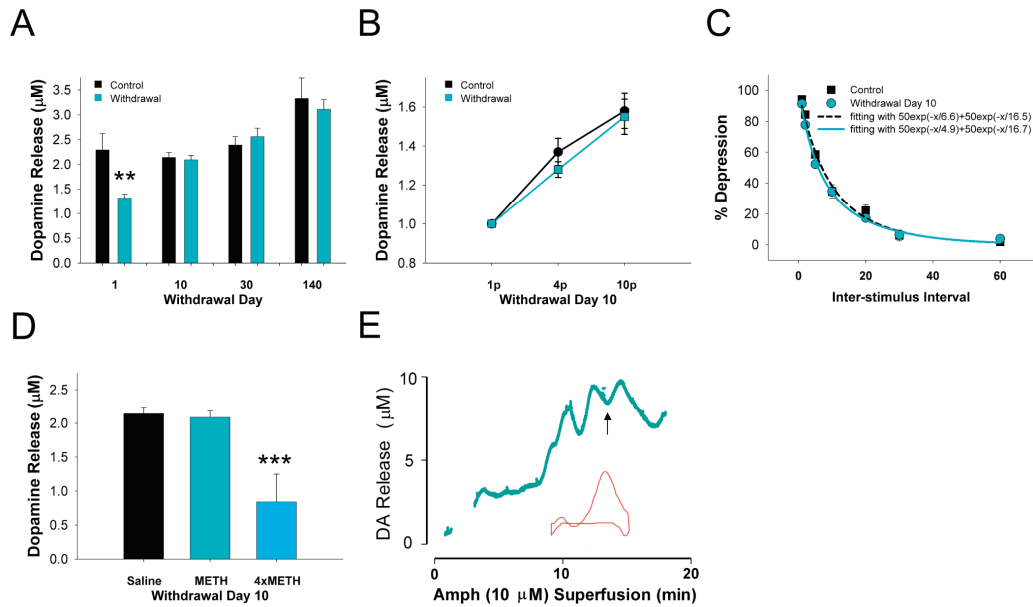


**Supplemental figure 1** - Average release of FM1-43 over time from cortical terminals stimulated at 1 Hz, 10 Hz, and 20 Hz following repeated saline (A – C) or methamphetamine (D – F; 20 mg/kg/day, 10 days) on withdrawal day 10. Curves (red) demonstrate exponential fitting for first-order kinetics. Curves were fit with:  $A=A_0 * \text{EXP}(-x/t)$ ;  $x=\ln(0.5) / t_{1/2}$ . For all comparisons  $p < 0.001$ ,  $r^2 > 0.99$ .



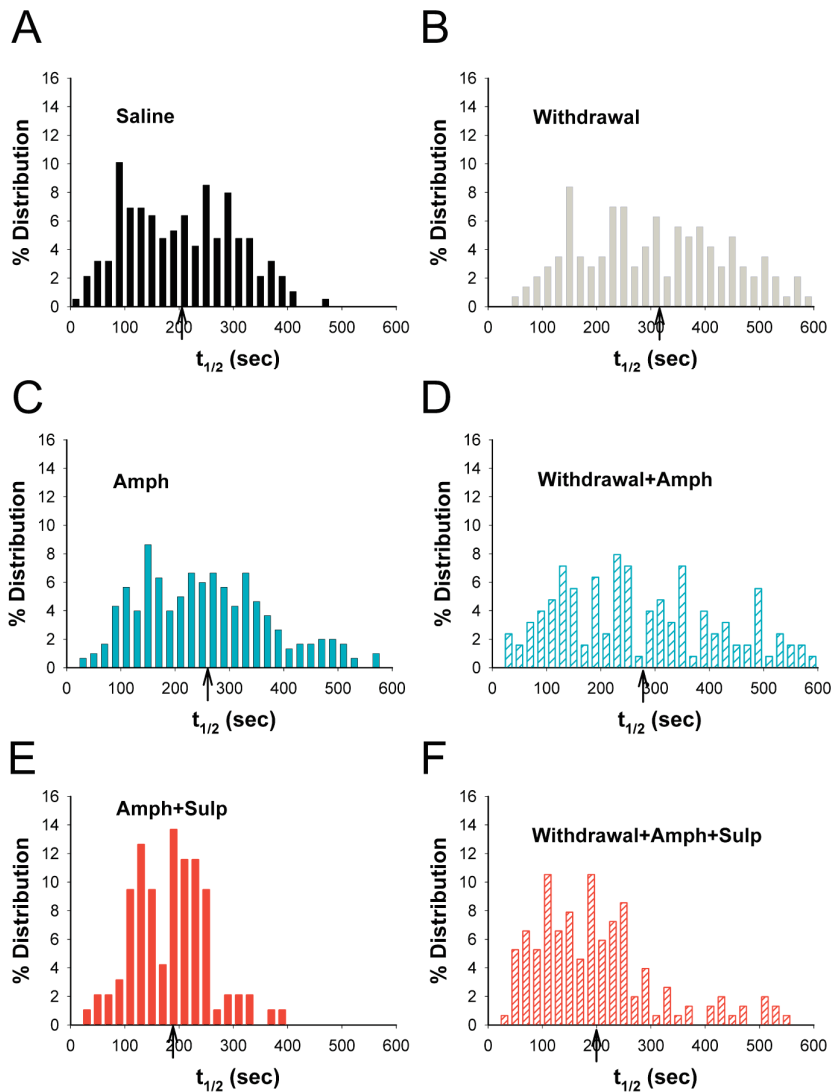
**Supplemental figure 2** – Fractional release of FM1-43. The fractional release parameter  $f$ , was calculated from  $\ln(F_1/F_2)/\Delta AP$  (Isaacson and Hille, 1997) where  $\ln$  is the natural logarithm,  $F_1$  and  $F_2$  are the fluorescent intensities at  $t_1$  and  $t_2$  respectively, and  $\Delta AP$  is the number of action potentials delivered during that period.

The mean fractional destaining per stimulus ( $f$ ) at 1 Hz was  $0.20 \pm 0.02\%$ , similar to previous reports (Bamford et al., 2004; Isaacson and Hille, 1997). Consistent with our previous investigations (Bamford et al., 2004), there was a marked frequency-dependent depression of FM1-43 destaining in slices from saline-treated mice (control), so that the mean fractional destaining per stimulus declined to  $f = 0.037 \pm 0.004\%$  at 10 Hz and  $f = 0.018 \pm 0.0001\%$  at 20 Hz ( $p < 0.001$ ,  $F_{(2, 90)} = 42.03$ , ANOVA). 10 days following repeated methamphetamine (withdrawal), the mean fractional destaining per stimulus ( $f$ ) at 1 Hz was  $0.20 \pm 0.01\%$ , with subsequent frequency-dependent depression to  $f = 0.018 \pm 0.001\%$  at 10 Hz and  $f = 0.012 \pm 0.001\%$  at 20 Hz ( $p < 0.001$ ,  $F_{(2, 90)} = 42$ , ANOVA). Fractional destaining was significantly reduced following repeated methamphetamine ( $p < 0.001$ ,  $F_{(2, 182)} = 203.65$ , two-way ANOVA) with the greatest depression seen at 10 Hz cortical stimulation ( $n = 31$ ;  $***p < 0.001$ ,  $t$ -test).



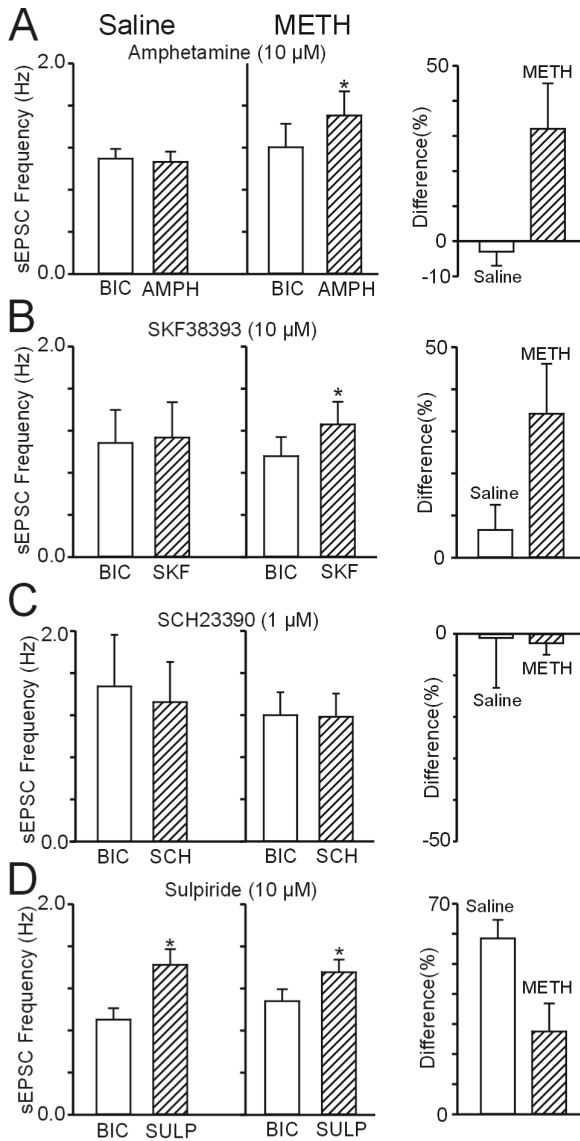
**Supplemental figure 3** – Dopamine efflux is normal following repeated methamphetamine (METH). **(A)** Electrically evoked dopamine release in response to a single pulse stimulus (1p) did not differ significantly between slices from saline- (control) and METH-treated mice (withdrawal), except for withdrawal day 1 (n=10, 9, 10, 3 slices for controls and 18, 18, 13, 6 slices for withdrawal mice on withdrawal day 1, 10, 30 and 140 respectively; \*\*p<0.01, paired *t*-test). **(B)** Evoked dopamine release normalized to that elicited by 1p stimulation for saline- (n=7 slices) and METH-treated mice (n=12 slices) on withdrawal day 1, 10, 30, or 140. Only data for withdrawal day 10 is shown. **(C)** Paired pulse depression was not altered following repeated METH on withdrawal day 10. Paired electrical stimuli were applied at variable interpulse intervals (1, 2, 5, 10, 20, 30 and 60 sec). Average time courses for recovery of the peak dopamine response are presented as the percent depression of the second stimulus response relative to the first (100 x [1 - second peak amplitude/first peak amplitude]) in controls and withdrawal mice. Data were fitted by double exponential functions (dashed lines) in

the form of  $y = 50 \times \exp(-t/\tau_f) + 50 \times \exp(-t/\tau_s)$ ;  $\tau_f$ , fast component time constant;  $\tau_s$ , slow component time constant. **(D)** Dopamine release in response to 1p stimulation was not altered in withdrawal mice on day 10 (n=18 slices) compared to controls (n=9 slices), whereas dopamine release was greatly decreased following a neurotoxic injection protocol (4 x METH, n=7 slices; \*\*\*p<0.001, paired *t*-test). **(E)** Cyclic voltammetry recordings of dopamine (DA) efflux by continuous amphetamine (AMPH) superfusion (10  $\mu$ M) beginning at time t=0. The background-subtracted voltammograms taken at point (arrow) identify dopamine and serve for calibration.



**Supplemental figure 4** - Histograms show distributions of  $t_{1/2}$  values on withdrawal day 10 following repeated saline (A, C, E) or methamphetamine (B, D, F; METH; 20 mg/kg/day, 10 days). (A) In slices from saline-treated mice, arrows, which indicate mean  $t_{1/2}$  values shift to the right (slower release) following an amphetamine (AMPH) challenge *in vitro* (C) and to the left (more rapid destaining) following exposure to both AMPH and the D2 receptor antagonist sulpiride (SULP) (E). (B) Repeated methamphetamine inhibits release in withdrawal with paradoxical presynaptic

potentiation (PPP) in release following an AMPH challenge *in vitro* (**D**). (**F**) In the presence of AMPH *in vitro*, D2 receptor blockade by Sulp enhances PPP to reverse chronic presynaptic potentiation (CPD).



**Supplemental figure 5** – Paradoxical presynaptic potentiation (PPP) in medium spiny neurons. Bar graphs represent average frequency of spontaneous (s) EPSCs in saline- (left column) and methamphetamine (METH)-treated (middle column) mice before (solid bars) and after (hatched bars) different drug treatments. Bar graphs on the right represent the percentage change in frequency produced after drug treatment. (A) Whereas amphetamine (AMPH) induced a small reduction in the frequency of sEPSCs in cells from saline-treated animals, it significantly increased their frequency in cells

from METH-treated animals. **(B)** Similarly, whereas the D1 receptor agonist SKF38393 produced only a modest increase in frequency in cells from saline-treated mice, it significantly increased the frequency in cells from METH-treated mice. **(C)** The D1 receptor antagonist SCH23390 produced no change in sEPSC frequency and **(D)** the D2 receptor antagonist sulpiride increased the frequency in cells from both groups. However, the increase was larger in cells from saline- compared to METH-treated animals. Student's *t*-tests or ANOVAs were used for group comparisons. Asterisks indicate the differences were statistically significant.



## SUPPLEMENTAL EXPERIMENTAL PROCEDURES

### Behavioral protocol

Animals were housed together on arrival in a colony room with a 12 hr light /dark cycle and were allowed *ad libitum* access to food and water except during locomotor recording. Locomotor responses were determined using animal activity monitor cages (San Diego Instruments). Four infrared beams separated by 8.8 cm, cross the width of each chamber, with the chambers connected to an IBM computer, which recorded the number of times each beam was broken. Locomotor activity was measured in ambulations (2 consecutive beam interruptions) summated over 5 min intervals. On each test day, animals were acclimated to individual activity chambers for 90 min to allow the animal to become accustomed to its behavioral cage before subsequent injections of either drug or saline. Following the injection, each animal was placed back into their respective activity chamber and ambulations were recorded over 90 min. To separate the effects of novelty from the pharmacological effects of the drug, animals were acclimated to the locomotor chambers and injected with saline for two days prior to each challenge. Since repeated challenges with amphetamine induced a progressive increase in the number of ambulations, locomotor responses to an amphetamine challenge were also compared between mice receiving repeated methamphetamine and repeated saline. Amphetamine was used as the challenge drug since equivalent doses of methamphetamine may induce stereotypy (not shown).

### FM1-43 loading and unloading

Coronal striatal sections (200  $\mu$ m) containing the cortex were cut on a vibratome and allowed to recover for 1 hr in carbogenated (95% O<sub>2</sub>, 5% CO<sub>2</sub>) artificial CSF solution (aCSF: (in mM) NaCl 109, KCl 5, NaHCO<sub>3</sub> 35, NaHPO<sub>4</sub> 1.25, MgCl<sub>2</sub> 1.2, CaCl<sub>2</sub> 2, HEPES acid 20, D-Glucose 10, pH 7.3-7.4, 295-305 mOs) at room temperature. Experiments were performed on the second to fourth frontal slice of caudate putamen

[Bregma, +1.54 to +0.62 mm] (Paxinos and Franklin, 2005). During experiments, slices were maintained in a RC-27L incubation chamber (56  $\mu$ l/ mm; Warner Instruments, Hamden, CT) perfused at 2 ml/min with carbogenated aCSF at 37°C.

FM1-43 (Invitrogen, Carlsbad, California; 8  $\mu$ M in aCSF) was loaded into presynaptic terminals by a 10 min train of 200- $\mu$ s, 400- $\mu$ A pulses at 10 Hz, applied to cortical layers V-VI by bipolar twisted tungsten electrodes, as described (Bamford et al., 2004). Electrical stimulation was provided by a Tektronix R564B wave generator (Tektronics, Gaithersburg, MD) through a stimulation isolator (AMPI, Jerusalem, Israel) and monitored by a S88 storage oscilloscope (Grass-Telefactor, West Warwick, RI). To remove adventitious tissue staining after FM1-43 loading, sections were incubated in ADVASEP-7 (AD7; CyDex, Overland Park, KS; 1 mM in aCSF) (Kay et al., 1999) for 2 min. During unloading, aCSF was supplemented with AD7 (100  $\mu$ M) and the AMPA receptor blocker NBQX (10  $\mu$ M; AG Scientific, San Diego, CA) to prevent recurrent endocytosis of dye into terminals and feedback synaptic transmission, respectively.

### **Imaging and data analysis**

Corticostriatal terminals labeled with the fluorescent tracer FM1-43 (Betz and Bewick, 1992; Ryan et al., 1993) were visualized in real time using the a Zeiss LSM 510 NLO multiphoton laser scanning confocal microscope equipped with a titanium-sapphire laser (excitation 810 nm/emission 650 nm) and a Plan-Neofluar 40 X/1.3 oil objective (Zeiss). Multiphoton microscopy provides excellent three-dimensional spatial resolution in brain slice preparations with minimal photo bleaching and photo damage (Mainen et al., 1999). Images were captured in 8-bit, 123 x 123  $\mu$ m regions of interest at 512-x 512 pixel resolution and acquired at 21.5 sec intervals. The striatal region of interest containing fluorescent puncta was 1.5 - 2.0 mm distant from the cortical stimulation electrodes. To compensate for any minor z-axis shift, a z-series of five images,

separated by 1  $\mu\text{m}$  in the z-plane, was obtained for each period. Images in each z-series were aligned and condensed with maximum transparency.

The time projection of images was analyzed for changes in puncta fluorescence using Image J (Wayne Rosband, National Institutes of Health, Rockville, MD) and custom-written software in interactive data language (IDL, Research Systems, Boulder, Colorado). The custom software adopts an object recognition protocol that rapidly processes terminal destaining (Bamford et al., 2004; Zakharenko et al., 2001). The software identifies spherical puncta 0.5 – 1.5  $\mu\text{m}$  in diameter that fluoresce two standard deviations above the background. Each puncta is aligned in the x, y, and z plane to prevent spatial drift and the time-dependent fluorescence intensity of each puncta is displayed graphically. Background fluorescence (<5%) was subtracted and the destaining half-time determined using a graphical software algorithm derived on SigmaPlot software (SPSS, Chicago, IL). Puncta demonstrating no active destaining were rejected.

### **Electrochemical recordings with cyclic voltammetry**

Striatal dopamine release was studied in 3-5 pairs of methamphetamine treated mice and their saline controls for each withdrawal day, i.e., day 1, day 10, day 30, and day 140, using fast-scan cyclic voltammetry. For neurotoxicity controls, some mice were treated with methamphetamine 10 mg/kg i.p. 4x at 2 hr intervals, a protocol well demonstrated to cause neurotoxicity for dopamine terminals (Matuszewich and Yamamoto, 2004; Thomas et al., 2004). Recordings were obtained from the first three coronal slices (300  $\mu\text{m}$ ), prepared from rostral caudate putamen. To minimize the variations of evoked dopamine release due to the heterogeneous distribution of the dopamine terminals, three sites in the dorsal striatal region of each slice were examined and the results averaged. Slices were allowed to recover for 1.5 hr in a holding chamber in oxygenated artificial cerebrospinal fluid (aCSF) at room temperature, and then placed in a recording

chamber, and superfused (1 ml/min) with aCSF (in mM: NaCl 125, KCl 2.5, NaHCO<sub>3</sub> 26, CaCl<sub>2</sub> 2.4, MgSO<sub>4</sub> 1.3, KH<sub>2</sub>PO<sub>4</sub> 0.3, D-glucose 10) at 36°C.

Electrochemical recordings and electrical stimulation were adapted from (Schmitz et al., 2001). Briefly, disk carbon fiber electrodes of 5- $\mu$ m diameter with a freshly cut surface were placed into the dorsal striatum about 50  $\mu$ m into the slice. For cyclic voltammetry, a triangular voltage wave (-400 to +900 mV at 280 V/s versus Ag/AgCl) was applied to the electrode every 100 ms. Current was recorded with an Axopatch 200B amplifier (Axon Instrument, Foster City, CA), with a low-pass Bessel Filter setting at 5 kHz, digitized at 25 kHz (ITC-18 board, Instrutech Corporation, Great Neck, New York). Triangular wave generation and data acquisition were controlled by a PC computer running a locally written IGOR program (Dr. E. Mosharov, Columbia University; WaveMetrics, Lake Oswego, OR). Striatal slices were electrically stimulated every 2 minutes with either a single pulse stimulation, a paired stimulus, or train stimulation at 100 Hz by an Iso-Flex stimulus isolator triggered by a Master-8 pulse generator (A.M.P.I., Jerusalem, Israel) using a bipolar stimulating electrode placed at  $\sim$ 100  $\mu$ m distance from the recording electrode. Background-subtracted cyclic voltammograms served to identify the released substance. The dopamine oxidation current was converted to concentration based upon a calibration of 5  $\mu$ M dopamine in aCSF after the experiment.

### **Detection of striatal acetylcholine (ACh) concentrations**

Mice treated with repeated saline or methamphetamine (20 mg/kg/day, 10 days) were sacrificed by decapitation on withdrawal day 10. Severed heads were immediately positioned in the center of a commercial microwave oven (Power output: 750 W) and irradiated for 3.0 sec (Bertrand et al., 1994). Striatum were immediately dissected from the brain and stored at -80°C. ACh tissue concentrations were determined as described (Damsma et al., 1985) by high performance liquid chromatography, based on a reaction

with acetylcholinesterase and choline oxidase (Vanderbilt Kennedy Center, Vanderbilt, TN). Both of these enzymes were bound to the stationary in post column immobilized enzyme reactor (IMER). In the assay, the tissue extracts were injected onto the HPLC ACh column (Bioanalytical Systems, West Lafayette, Indiana) that resolved ACh and choline. As each analyte departed from the column they entered the IMER, which converted ACh to Ch by acetylcholinesterase, and was further oxidized by choline oxidase to produce hydrogen peroxide. This reaction product was then detected amperometrically and quantitated on a glassy carbon-working electrode (+500 mV). The HPLC system is composed of a Waters 717+ autosampler, Water model 515 pump and Antec Decade electrochemical detector. Tissue samples were homogenized in 250- $\mu$ l acetonitrile using a sonic dismembrator. Samples were centrifuged at 13000 g for 30 min. Acetonitrile fraction was transferred to a clean tube and washed twice with 125- $\mu$ l heptane. Acetonitrile layer was then evaporated using a stream of nitrogen. 75  $\mu$ l of the HPLC mobile phase (37.5 mM  $\text{H}_3\text{PO}_4$ , pH 8.5) was added to the dried tube and vortexed. 50  $\mu$ l of the sample was then injected into the equilibrated HPLC.

### **Electrophysiology**

Saline- or methamphetamine-treated animals were deeply anesthetized with halothane and sacrificed. The brains were dissected and placed in oxygenated ice-cold low  $\text{Ca}^{2+}$  artificial cerebrospinal fluid (aCSF) containing (in mM): 130 NaCl, 1.25  $\text{NaH}_2\text{PO}_4$ , 26  $\text{NaHCO}_3$ , 5  $\text{MgCl}_2$ , 1  $\text{CaCl}_2$ , and 10 D-glucose. Coronal slices (350  $\mu$ m) were cut and transferred to an incubating chamber containing normal aCSF (with 2 mM  $\text{CaCl}_2$  and 2 mM  $\text{MgCl}_2$ ) oxygenated with 95%  $\text{O}_2$ -5%  $\text{CO}_2$  (pH 7.2-7.4, 290-310 mOsm,  $25\pm 2^\circ\text{C}$ ). After 1 hr, slices were placed on the stage of an upright fixed-stage Olympus microscope (BX51), submerged in continuously flowing aCSF (4 ml/min). Whole-cell patch clamp recordings in voltage clamp mode were obtained from medium spiny neurons visualized in slices with the aid of infrared videomicroscopy (Cepeda et al.,

1998; Wu et al., 2007). Medium spiny neurons were identified by somatic size and typical basic membrane properties (input resistance, membrane capacitance and time constant). Series resistance was  $<25 \text{ M}\Omega$  and was compensated 70-80%. The internal solution in the patch pipette (3-5  $\text{M}\Omega$ ) contained (in mM): Cs-methanesulfonate 130, CsCl 10, NaCl 4,  $\text{MgCl}_2$  1, MgATP 5, EGTA 5, HEPES 10, GTP 0.5, phosphocreatine 10, leupeptin 0.1 (pH 7.25-7.3, 280-290 mOsm).

Spontaneous and evoked excitatory postsynaptic currents (EPSCs) were recorded in normal aCSF in the presence of bicuculline (BIC 10  $\mu\text{M}$ , a  $\text{GABA}_A$  receptor blocker) at a holding potential of -70 mV. In some slices the  $\text{Na}^+$  channel blocker, tetrodotoxin (1  $\mu\text{M}$ ) was added to isolate miniature (m) EPSCs. Spontaneous (s) EPSCs were recorded for 3-6 min. The membrane current was filtered at 1 kHz and digitized at 100  $\mu\text{s}$  using Clampex (gap free mode) (Axon Instruments, Inc.; Foster City, CA). Spontaneous synaptic events were analyzed off-line using the Mini Analysis Program (Jaejin Software, Leonia, NJ). This software was used to calculate EPSC frequency, amplitude of events, and to construct amplitude-frequency and cumulative probability histograms. The threshold amplitude for the detection of an event was adjusted to at least 2 times above root mean square noise level ( $\sim 2\text{-}3 \text{ pA}$  at -70 mV). Frequencies were expressed as number of events per second (Hz). Synaptic currents also were evoked by electrical stimulation of the deep cortical layers just above the corpus callosum using a bipolar tungsten electrode. Current pulses (0.1 ms duration) at stimulation strengths ranging from 0.1 to 1.0 mA were delivered at 30 sec intervals. Threshold current required to induce an EPSC, response amplitude and kinetics were measured for every cell.

## **SUPPLEMENTAL REFERENCES**

Bamford, N. S., Zhang, H., Schmitz, Y., Wu, N. P., Cepeda, C., Levine, M. S., Schmauss, C., Zakharenko, S. S., Zablow, L., and Sulzer, D. (2004). Heterosynaptic

dopamine neurotransmission selects sets of corticostriatal terminals. *Neuron* 42, 653-663.

Bertrand, N., Beley, P., and Beley, A. (1994). Brain fixation for acetylcholine measurements. *J Neurosci Methods* 53, 81-85.

Betz, W. J., and Bewick, G. S. (1992). Optical analysis of synaptic vesicle recycling at the frog neuromuscular junction. *Science* 255, 200-203.

Cepeda, C., Colwell, C. S., Itri, J. N., Chandler, S. H., and Levine, M. S. (1998). Dopaminergic modulation of NMDA-induced whole cell currents in neostriatal neurons in slices: contribution of calcium conductances. *J Neurophysiol* 79, 82-94.

Damsma, G., Westerink, B. H., and Horn, A. S. (1985). A simple, sensitive, and economic assay for choline and acetylcholine using HPLC, an enzyme reactor, and an electrochemical detector. *J Neurochem* 45, 1649-1652.

Isaacson, J. S., and Hille, B. (1997). GABA(B)-mediated presynaptic inhibition of excitatory transmission and synaptic vesicle dynamics in cultured hippocampal neurons. *Neuron* 18, 143-152.

Kay, A. R., Alfonso, A., Alford, S., Cline, H. T., Holgado, A. M., Sakmann, B., Snitsarev, V. A., Stricker, T. P., Takahashi, M., and Wu, L. G. (1999). Imaging synaptic activity in intact brain and slices with FM1-43 in *C. elegans*, lamprey, and rat. *Neuron* 24, 809-817.

Mainen, Z. F., Maletic-Savatic, M., Shi, S. H., Hayashi, Y., Malinow, R., and Svoboda, K. (1999). Two-photon imaging in living brain slices. *Methods* 18, 231-239, 181.

Matuszewich, L., and Yamamoto, B. K. (2004). Chronic stress augments the long-term and acute effects of methamphetamine. *Neuroscience* 124, 637-646.

Paxinos, G., and Franklin, J. (2005). *The Mouse Brain in Stereotaxic Coordinates*, Second edn (London, Academic Press).

Ryan, T. A., Reuter, H., Wendland, B., Schweizer, F. E., Tsien, R. W., and Smith, S. J. (1993). The kinetics of synaptic vesicle recycling measured at single presynaptic boutons. *Neuron* 11, 713-724.

Schmitz, Y., Lee, C. J., Schmauss, C., Gonon, F., and Sulzer, D. (2001). Amphetamine distorts stimulation-dependent dopamine overflow: effects on D2 autoreceptors, transporters, and synaptic vesicle stores. *J Neurosci* 21, 5916-5924.

Thomas, D. M., Walker, P. D., Benjamins, J. A., Geddes, T. J., and Kuhn, D. M. (2004). Methamphetamine neurotoxicity in dopamine nerve endings of the striatum is associated with microglial activation. *J Pharmacol Exp Ther* 311, 1-7.

Wu, N., Cepeda, C., Zhuang, X., and Levine, M. S. (2007). Altered corticostriatal neurotransmission and modulation in dopamine transporter knock-down mice. *J Neurophysiol* 98, 423-432.

Zakharenko, S. S., Zablow, L., and Siegelbaum, S. A. (2001). Visualization of changes in presynaptic function during long-term synaptic plasticity. *Nat Neurosci* 4, 711-717.